# 6

# Magnetic Resonance Angiography of Aortic Diseases in Children

Shobhit Madan, Soma Mandal and Sameh S. Tadros
*Division of Pediatric Radiology*
*Department of Radiology*
*Children's Hospital of Pittsburgh of UPMC*
*University of Pittsburgh School of Medicine*
*Pittsburgh, PA*
*USA*

## 1. Introduction

Magnetic resonance angiography (MRA), a non-invasive, radiation-free imaging technique dependent on the body's natural magnetic properties in blood vessels, investigates abnormalities within the aorta. MRA is generally divided into Gadolinium (Gd) based contrast enhanced MRA (CE-MRA) and non-contrast enhanced MRA (NCE-MRA), used for both qualitative and quantitative assessment of the aorta. These sequences can be exemplified with a variety of aortic abnormalities including aortic dissection, coarctation of the aorta, genetic disorders with aortic pathologies (e.g., Marfan's syndrome, Loeys-Dietz syndrome), ascending and descending aortic aneurysms, Takayasu Arteritis, and various anomalies concerning the aortic arch as well as the aortic valve. While MRA can be applied to nearly any vessel in the body, the primary objective of this chapter is to focus on the role of MRA in the accurate quantitative and qualitative assessment of congenital and acquired aortic diseases. In many hospitals, a significant number of patients who are referred to MRA imaging is comprised of patients with aortic diseases, especially coarctation of aorta [Taylor, 2008]. The diagnostic utility of MRA is illustrated by a variety of pediatric aortic abnormalities.

## 2. Magnetic resonance angiography sequences

Examination of the aorta can be classified under purely qualitative imaging and both qualitative and quantitative imaging.

### 2.1 Qualitative aortic angiography

The first basic sequence employed is the non-electrocardiographic (ECG) gated steady–state free precision (SSFP) localizers in the coronal, axial and sagittal planes to visualize the entire chest and upper abdomen, providing a basic overview of cardiac and visceral situs and cardiovascular anatomy (Figure 1A-C). The localizers serve as the starting point for further disease-specific multiplanar image acquisition of the aorta for morphological, functional,

and hemodynamic evaluation. Black-blood imaging, where the flowing blood appears dark and general aortic anatomy can be assessed, is exclusively used for qualitative analysis of the aortic morphology in multiple planes (Figure 1D-F). Black blood imaging includes a T1-weighted spin echo sequence (which allows for rapid aortic morphological assessment at low spatial resolution) followed by a double inversion recovery spin echo sequence (which allows for high spatial resolution and improved blood-myocardium contrast) in order to characterize cardiovascular tissue and assess airway obstruction.

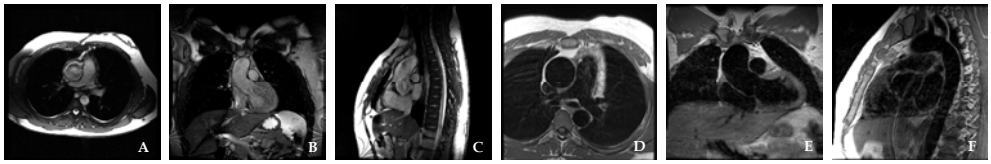


Fig. 1. SSFP localizer images demonstrating the aorta in axial (A), coronal (B), and sagittal (C) planes; Black-blood images demonstrating the aorta in axial (D), coronal (E), and sagittal (F) planes.

### 2.2 Quantitative & qualitative aortic angiography

In assessing the aorta both qualitatively and quantitatively, the cardiac imager may have two intentions in the quantitative measurement of vessels. On one hand, the imager can measure hemodynamic parameters such as blood flow, which would be accomplished more thoroughly by sequences which are concerned with functional assessment. On the other hand, more static measurements, such as assessing aortic root dilatation, would be accomplished more readily with sequences dedicated to morphological assessment. The following qualitative and quantitative sequences are discussed below.

**Functional Assessment**

A popular sequence used for functional assessment is the SSFP cine white blood imaging sequence, which provides superior quantitative imaging of the aorta and its branch vessels [Finn et al., 2006] without the use of contrast agents with high temporal resolution in multiple planes (Figure 2).

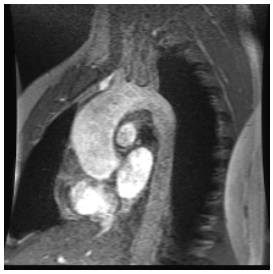

Fig. 2. SSFP cine image demonstrating aorta in a sagittal plane.

SSFP imaging is very useful in qualitative assessment of aortic valve for regurgitation and stenosis. This technique requires breath-hold which is necessary to improve image quality by avoiding motion artifacts. Post processing of SSFP images includes assessment of 3D

computational fluid dynamics (CFD). CFD simulation of hemodynamics in aortic arch models allows for quantification of high resolution internal flow fields (e.g. velocity, pressure) as well as useful flow derived parameter such as time resolved wall shear stress, energy dissipation and power loss (Figure 3). Flow derived parameters have application in surgical planning and post-operative assessment of hemodynamic efficiency in surgical anastomosis or venous flow confluences [Lara et al., 2011]. CFD is a powerful tool for simulation of altered hemodynamics in pathological anatomies and may be used to assess aortic arch abnormalities, severity of coarctation (via assessment of pressure gradients, collateral flow, and velocity across the coarctation), and flow in arch anomalies (e.g. hypoplastic arch).

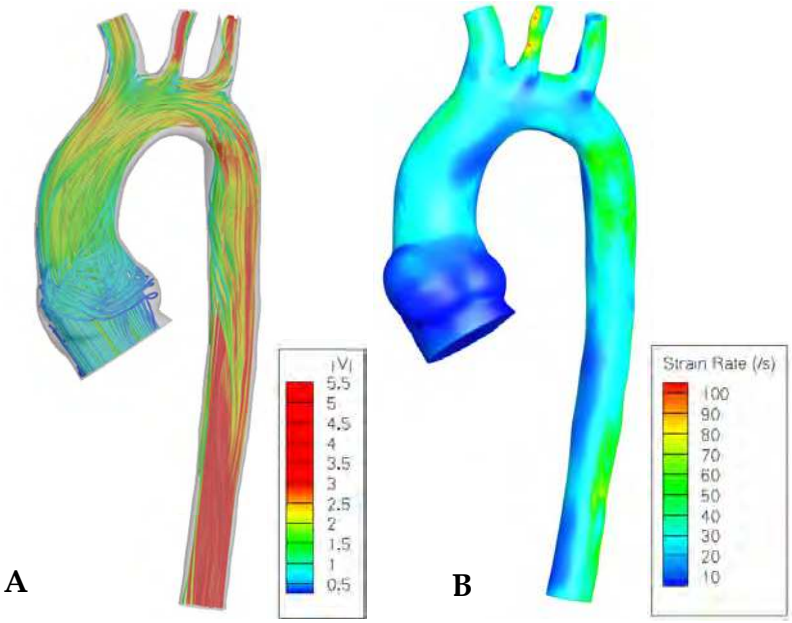


Fig. 3. Cine MRI based surface model reconstructions of a normal neonatal arch [Pekkan et al. 2008] were used to conduct 3D CFD and assess vascular flow. (A) Streamlines colored by inlet normalized velocity magnitude, |V|, for a mean steady aortic root velocity of 0.33 m/s; B) Wall shear strain rate, with an observed stain rate is within normal ranges for neonatal flow.

Another functional imaging sequence is velocity-encoded cine phase contrast imaging (Figure 4). Phase contrast imaging is a method of obtaining quantitative information on blood flow, in addition to providing anatomic imaging of vessels. Its mechanics depend on magnetic moments, or spins, which ultimately shift in their phase of rotation, allowing for a voxel specific velocity to be calculated and an image to be formed [Lotz et al., 2002; Sena 2008]. Quantification of flow at multiple levels of the aorta can be performed with and without breath holding using this technique. Determination of collateral flow, velocity, and pressure gradient across the coarctation in patients with coarctation of aorta can be preformed using this MR technique.

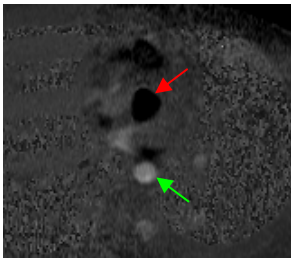

Fig. 4. Phase contrast image of the aorta demonstrating flow in the ascending aorta (red arrow) and descending aorta (green arrow) which is quantifiable as demonstrated in Figure. 14D later in the chapter.

**Morphological Assessment**

Traditional imaging of MRA includes both Gd-based CE-MRA as well as NCE-MRA using 3D SSFP, both of which serve as the source images for further post-processing which allows for static measurements and the creation of 3D models.

Gd-based CE-MRA has certain technical advantages over non-contrast enhanced MRA including superior visualization of vasculature, shorter acquisition times, and being less prone to alteration by motion artifacts [Hartung et al., 2011]. CE-MRA is considered the most quick and efficient way of illustrating the entire thoracic vasculature (Figure 5A); high resolution spatial techniques within this sequence are especially beneficial in imaging the small vasculature of newborns with specific aortic malformations like truncus arteriosus [Sena et al., 2008]. The ability to reconstruct maximum intensified projection (MIP) images (Figure 5B), volume rendered (VR) images (Figure 5C), and curved planar reformatted images allows for accurate measurements of vascular dimensions and aortic anatomy in patients with congenital and acquired aortic diseases. Limitations of CE-MRA techniques include the presence of motion artifacts in patients unable to breath-hold and patients with history of contrast agent allergies. A long-term complication of Nephrogenic Systemic Fibrosis in patients with poor renal function is another limitation of CE-MRA. Patients with metabolic syndromes, diabetes, and renal disease are especially at high risk and complications in these patients have spurred research with more diluted doses of contrast agents [Perazella et al., 2009].

With recent technical advancements in aortic imaging, NCE-MRA using 3D SSFP with and without breath hold imaging aids in the qualitative and quantitative assessment of the aorta with excellent spatial resolution without the need for Gd based contrast agents (Figure 5D). This advanced cardiovascular MRA sequence is especially useful in patients with a contraindication to contrast agents or who are unable to hold their breath. Measurements of the aorta and its branch vessels along with 3D and MIP image reconstructions in multiple planes are also possible with high accuracy using this sequence. A type of NCE-MRA, which will not be discussed in this chapter, is time of flight (TOF) MRA, which is based off of inflow effects, is a technique which is limited by longer acquisition time and a higher incidence of artifacts.

Additionally, late gadolinium enhancement (LGE) is a method by which regions of inflammation and fibrosis in the wall of aorta and its branch vessels can be identified. LGE,


Fig. 5. CE-MRA coronal image (A), MIP sagittal reconstruction of CE-MRA (B), VR sagittal reconstruction of CE-MRA (C), and axial NCE-MRA image using 3D SSFP (D) of the aorta. MIP and VR reconstructions are extremely useful for a qualitative overview of the vascular morphology for preoperative assessment.

a sequence that visualizes fibrotic or infarcted heart tissue, derives its name from the fact that there is a delay in the washout of gadolinium-based contrast because fibrotic regions are filled with collagen. It was first demonstrated in the late 1980s with animal models demonstrating enhancement of myocardial infarcts [van Dijkman et al., 1989]. In recent decades, LGE has been shown to be particularly useful in pediatric diseases [Prakash et al., 2003]. However, the exact mechanism of contrast agent localization in infarcted tissue is a debated topic [Finn et al., 2006].

As mentioned, MRA can be utilized to image nearly any vessel in the body. The following table is a concise summary of current MRA techniques used for imaging of various vessels in the body, with sequences like black blood, phase contrast, SSFP, and ECG-gated fast spin echo (which is a variation of SSFP which we have not discussed in the chapter due to its irregular and sparse use), which are specifically used for aortic imaging [Morita et al., 2011].

**Advantages, Limitations, and Clinical Applications of Unenhanced MR Angiographic Techniques**

| Technique | Advantages | Limitations | Clinical Applications |
|---|---|---|---|
| TOF | Simple and robust | Long imaging time; direction dependent; signal loss in in-plane, turbulent, or complex flow; susceptible to field heterogeneities | Cerebral arteries (3D), peripheral vessels (2D), head and neck arteries (2D) |
| Phase-contrast | Suppressed background signals, direction independent | Long imaging time (3D), signal loss in turbulent flow, sensitive to motion, parameter dependent | Cerebral veins (3D), hemodynamic evaluation |
| ECG-gated FSE | Relatively short imaging time, sensitive to slow flow, less susceptible to field heterogeneities | Complex imaging, direction dependent, sensitive to motion | Peripheral arteries, aorta |
| SSFP | Short imaging time, high signal-to-noise ratio, relatively flow independent | High background signals, susceptible to field heterogeneities | Renal arteries, aorta, coronary arteries |
| ASL with SSFP | High signal-to-noise ratio, suppressed background signals | Relatively complex imaging, signal loss in fast or complex flow, susceptible to field heterogeneities | Renal arteries, various visceral vessels |
| Black blood | Less sensitive to complex flow | Long imaging time, unsuitable for angiography | Vessel wall imaging, carotid arteries, aorta |

Note.—ASL = arterial spin labeling, ECG = electrocardiograph, FSE = fast spin echo, SSFP = steady-state free precession, 3D = three-dimensional, 2D = two-dimensional.

## 3. Diseases of the aorta

Various diseases of the aorta, primarily highlighted in the pediatric population due to the large volume of pediatric cases in our institution as well as the congenital presentation of most of the diseases, are illustrated with the sequences discussed above. In general, almost all aortic diseases will be imaged via black-blood, CE-MRA, SSFP, phase contrast, and post-processed to MIP and VR images as necessary for a comprehensive assessment available for the cardiac imager, cardiologist, or the surgeon.

### 3.1 Coarctation of aorta

Coarctation of aorta, a congenital condition characterized by aortic narrowing, is subtyped based on the location of the narrowing relative to the ductus arteriosus. The use of MRA in determining the severity of stenosis within aortic coarctation is well documented [Nielsen et al., 2005; Muzzarelli et al., 2011; Secchi et al., 2009]. Coarctation of aorta requires comprehensive qualitative and quantitative evaluation for the assessment of severity of coarctation (e.g. velocity measurements at the level of coarctation as well as pre- and post-coarctation). Morphological evaluation of coarctation (Figure 6) and functional assessment (Figure 7) of collateral flow at various levels of the descending aorta is routinely performed.

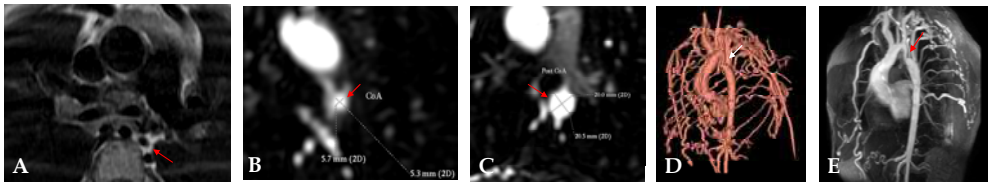


Fig. 6. Black blood axial T1 weighted image of coarctation (A), double oblique measurement of CE-MRA at coarctation demonstrating 73% stenosis (B), calculated by the distal to coarctation (C) measurement; VR (D) and MIP (E) images demonstrating aggressive collateral vessels due to severe coarctation of aorta.

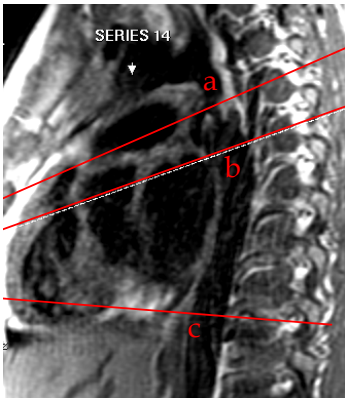


Fig. 7. Sagittal black blood image of aorta used as a precursor to phase contrast image acquisition at coarctation (a: velocity=2.2m/s), below coarctation (b: flow=27.3 ml/beat), and at hiatus (c: flow=47 ml/beat) with a collateral flow of 20 ml/beat; aortic flow.

### 3.2 Ascending & descending aortic aneurysm

Ascending and descending aortic aneurysms both arise from systemic and connective tissue diseases, including systemic hypertension, Marfan's syndrome, Loeys-Dietz syndrome, etc. (Figure 8). A weakness in the aortic wall causes distension leading to increased pressure and flow which may lead to other pathologies (e.g. aortic dissection as discussed later). Ascending and descending aneurysms are typically imaged quantitatively through CE-MRA along with overall qualitative assessment of bulging of the aortic wall.

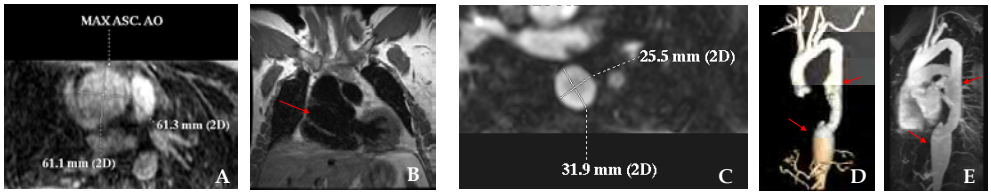


Fig. 8. (A) CE-MRA double oblique view of an ascending aortic aneurysm with an aortic diameter of ≈ 6 cm (normal is < 3.5 cm); (B) Black blood coronal image of ascending aortic aneurysm; (C) CE-MRA double oblique view of a descending thoracic aortic aneurysm with an aortic diameter of ≈ 2.8 cm; VR (D) and MIP (E) reconstructions of descending thoracic and abdominal aortic aneurysm.

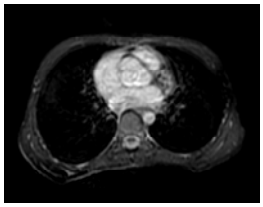

Loeys-Dietz syndrome is a genetic disorder which involves a high likelihood of ascending aortic aneurysms as well as aortic dissections (see below). A dilated aortic root is demonstrated in this patient with Loeys-Dietz using NCE-MRA; this technique is used frequently since regular follow-up of this disease is required and may minimize complications arising from contrast agents.

### 3.3 Aortic dissection

Aortic dissection, a malformation in which the inner aortic wall is torn and ultimately desecrated, is a life threatening condition. Generally, this defect is further subtyped according to the origin of the tear and to the extent certain areas of the aorta are involved. Within all these variations, MRA was considered the gold standard in detection and assessment of aortic dissections since the early 1990s due to nearly flawless sensitivity and specificity [Neinaber et al., 1993]. More recently, however, it has been shown that aortic dissection is diagnosed with equivalent reliability in a number of imaging modalities including echocardiography and computed tomography (Litmanovich et. al, 2009; Shiga et. al, 2006). Aortic dissection is typically sequenced via CE-MRA, SSFP, and phase contrast MRA, followed by post-processing of VR and MIP images, helping in delineating the extent of dissection and the flow within the true and false (which results from tearing) lumen.

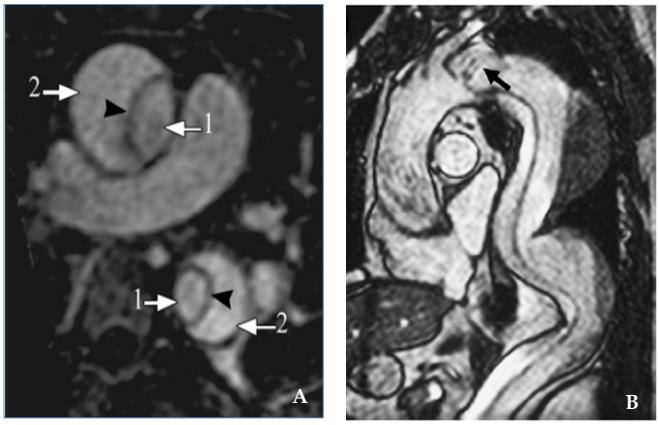


Fig. 9. (A) CE-MRA in an axial-oblique view demonstrating the true (1) and false (2) lumen within the ascending and descending aorta from Liu et al., 2007; (B) Sagittal SSFP demonstrates aortic dissection from Sakamoto et al., 2010.

### 3.4 Aortic arch malformations & vascular rings

In contrast to more innocuous forms of alternative aortic arch anatomy (Figure 10B), aortic arch malformations occur as congenital defects in the development of the aortic arch and great vessels. An example is hypoplastic aortic arch (Figure 10A), where narrowing of the aorta possibly leads to further complications. Vascular rings, which involve abnormal encircling of the trachea and/or esophagus by the aorta or its branches, include interrupted, double, and right aortic arches (Figures 11 & 12).

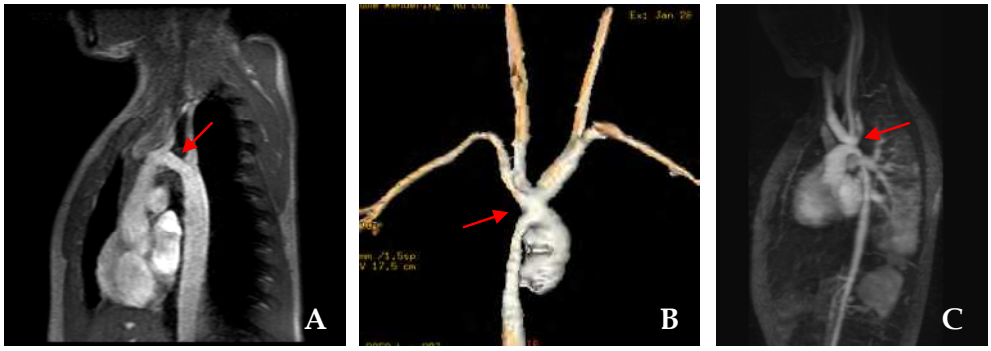


Fig. 10. (A) SSFP sagittal image demonstrating hypoplastic aortic arch; VR (B) and MIP (C) reconstructions demonstrating the common origin of neck vessels from the aortic arch.

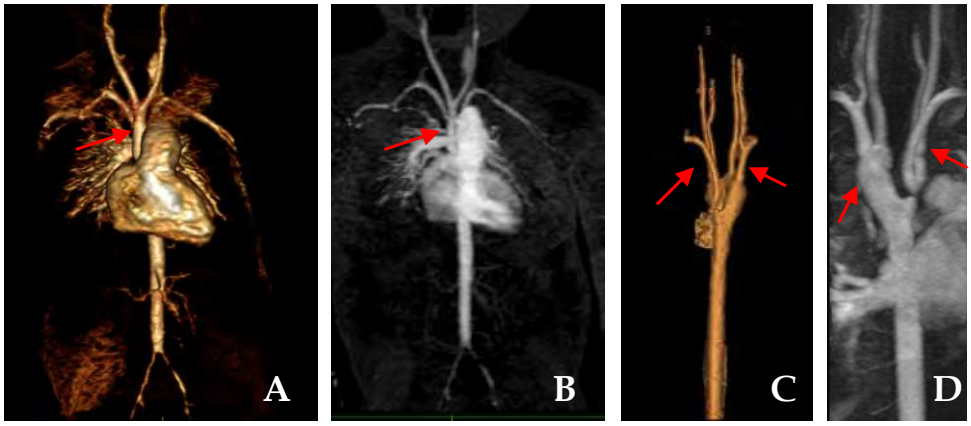


Fig. 11. VR (A) and MIP (B) reconstructions of the interrupted aortic arch anomaly; VR (C) and MIP (D) reconstructions of the double aortic arch with mirror image branching.

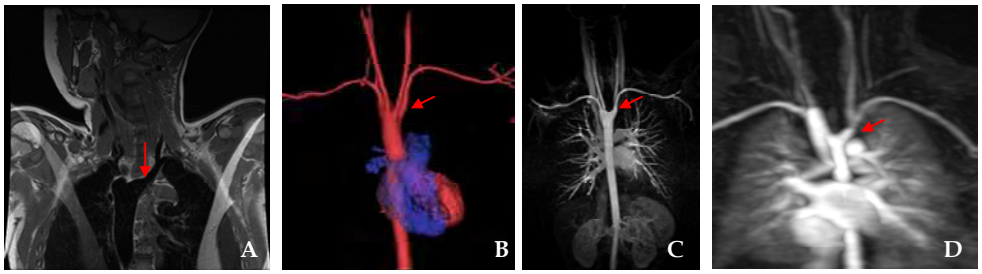


Fig. 12. (A) Coronal black-blood image demonstrating right aortic arch with aberrant left subclavian artery originating from the descending aorta; VR (B) and MIP (C) reconstructions of right aortic arch; (D) MIP image showing diverticulum of Kommerell giving rise to aberrant left innominate artery branching into left common carotid and left subclavian artery.

### 3.5 Aortic valve malformations: bicuspid & quadricuspid aortic valve

Bicuspid aortic valve is a defect in the aortic valve in which two leaflets exist instead of the characteristic three found between the left atrium and left ventricle (Figure 13C-E). While it may be innocuous initially, the bicuspid aortic valve can lead to complications such as calcifications and stenosis later in life with varying degrees of severity. MRA is an appropriate imaging modality for the exploration of this valvular defect, considering that imaging modalities like echocardiography may miss certain variations of bicuspid aortic valve [Piccoli et al., 2010]; additionally, recent research has been directed toward understanding the implications of flow dynamics within bicuspid aortic valve patients, a feature which only MRA can offer [Hope et al., 2010]. Similarly, a quadricuspid aortic valve is a defect in the aortic valve in which four leaflets exist instead of the characteristic three found between the left atrium and left ventricle (Figure 13A-B). It is typically imaged with a combination of modalities, with MRA being particularly useful in assessing regurgitation of the valve [Pouleur et al., 2009].

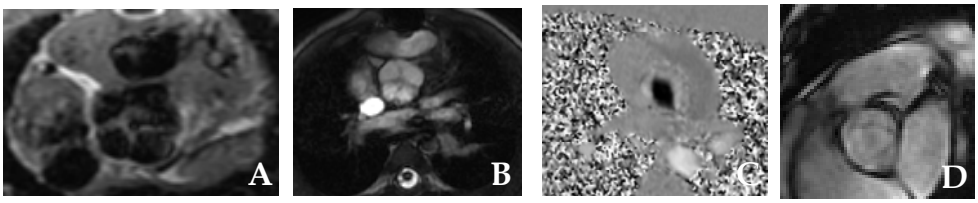


Fig. 13. Black-blood axial (A) and SSFP (B) image of quadricuspid aortic valve; Phase contrast (C) and SSFP (D) image of bicuspid aortic valve.

### 3.6 Aortic valve malformation: aortic stenosis & regurgitation

Aortic stenosis, or narrowing of the aortic valve, presents with a variety of problems dependent on the severity of valvular narrowing (Figure 14A-B). MRA has been shown to be a superior method, in terms of less intra- and inter- observer measurement variability, over echocardiography in the assessment of aortic stenosis severity [Garcia et al., 2011]. Aortic valve regurgitation results when the aortic valve insufficiently closes and allows blood to leak back into the left ventricle instead of completely entering the aorta (Figure 14C-D). While the aortic valve regurgitation is commonly first noticed by echocardiography, the assessment of the severity of aortic valve regurgitation and its effect on left ventricular function is done most sophisticatedly through MRA [Gabriel et al., 2011; Uretsky et al., 2010;].

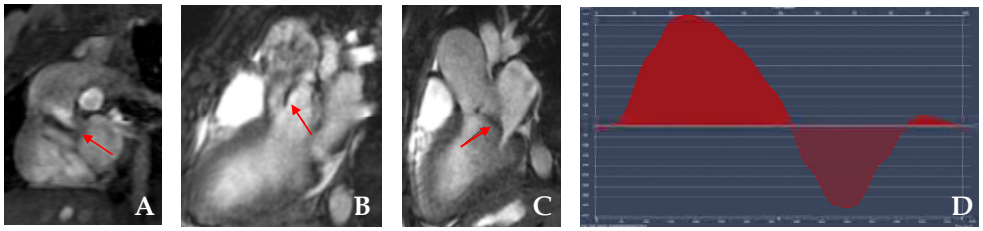


Fig. 14. (A) SSFP cine short axis and (B) left ventricular outflow tract view demonstrating an aortic stenotic jet with a velocity of 1.8m/s (normal being ≈ 1); (C) SSFP cine left ventricular outflow tract view demonstrating aortic regurgitation; (D) Quantification of aortic regurgitation fraction measuring 45%, a calculation made possible by phase contrast imaging at the level of the ascending aorta.

### 3.7 Aortic inflammatory disease: Takayasu arteritis

Takayasu Arteritis, an inflammatory disease which causes various types of stenosis, occlusion, and/or dilatation in the aorta, carries a significant risk of premature death (Figure 15). While MRA overall is a good diagnostic tool for the functional aspects of this multifaceted disease (Keenan et al., 2009), the feature of LGE is particularly useful in demonstrating scarring in Takayusu Arteritis patients.

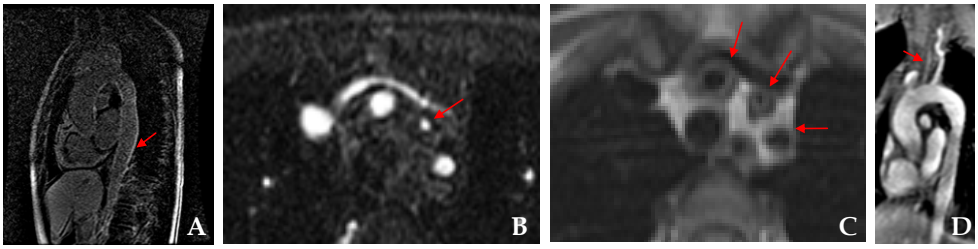


Fig. 15. (A) LGE image of the aorta in a sagittal plane demonstrating aortic wall enhancement, a marker of active inflammatory disease; (B) CE-MRA axial view of aortic arch branches demonstrating severe narrowing of the left common carotid artery measuring 2.2 mm; (C) Wall thickening also involves the 3 branches of the aortic arch, the right brachiocephalic, left common carotid and left subclavian artery with (D) long segment stenosis of the left common carotid artery.

## 4. Magnetic resonance angiography of other vessels

While not the main focus of this chapter, use of MRA extends to the coronary arteries and peripheral vessels as well. In terms of arterial stenosis within the coronary arteries, overall vessel diagnostic accuracy with MRA is approximately 73% sensitive and 86% specific, which is significantly lower than the nearly perfect visualization (approximately 98%) of the aorta as demonstrated with all of the aforementioned malformations [Miller et al., 2009]. Studies have shown computed tomography angiography to be more sensitive and specific than MRA in the visualization of coronary artery stenosis and detection of coronary artery disease [Dewey et al., 2006; Schuijf et al., 2006; Scheutz et al., 2010;]. In the case of peripheral arterial diseases, however, MRA has been shown to have superior diagnostic accuracy over computed tomography angiography in the visualization of peripheral vessels, such as those in the lower extremities [Menke et al., 2010].

## 5. Conclusion

As demonstrated by various qualitative and quantitative techniques, MRA has contributed to understanding features of aortic diseases within the pediatric population in particular. Through a range of sequencing which evaluates the morphological and functional aspects related to aortic malformations, MRA allows a comprehensive assessment of aortic disease in a sophisticated manner over other imaging modalities. MRA is a favorable imaging modality (as opposed to computed tomography) for the patient because of a lack of radiation and for the clinician due to its clinical applications with cardiovascular diseases and the ability to investigate both anatomy and function simultaneously with high resolution [Brenner et al., 2007; Finn et al., 2006]; however, there are some challenges with MRA in patients less than 8 years of age, where imaging requires children to be anesthetized in order to ensure appropriate breath-hold which is necessary to mitigate motion artifacts [Taylor, 2008]. When it comes to examining congenital heart diseases, MRA is still considered a superior diagnostic tool, as it is able to quantify particular lesions using flow measurements, a fundamental limitation within computed tomography.

## 6. Acknowledgements

We would like to thank the lead MR technologist, Dennis Willaman, and MR technologist Sara Carter at the Division of Pediatric Radiology at Children's Hospital of Pittsburgh of UPMC for acquiring MRA images. Also, we would like to thank Dr. Kerem Pekkan and Prahlad G. Menon from the Department of Biomedical Engineering at Carnegie Mellon University for contributing images related to computational fluid dynamics.

## 7. References

Brenner DJ, Hall EJ. Computed tomography - an increasing source of radiation exposure. *N Engl J Med.* 2007; 357: 2277-2284.

Dewey M, Teige F, Schnapauff D, Laule M, Borges AC, Wernecke KD, Schink T, Baumann G, Rutsch W, Rogalla P, Taupitz

Finn JP, Nael K, Deshpande V, Ratib O, Laub G. Cardiac MR imaging: state of the technology. *Radiology*. 2006; 241(2): 338-351.

Firmin, D. N. and Pennell, D. J. Integrated cardiac and vascular assessment in Takayasu arteritis by cardiovascular magnetic resonance. *Arthritis & Rheumatism*. 2009;60: 3501–3509.

Gabriel RS, Renapurkar R, Bolen MA, Verhaert D, Leiber M, Flamm SD, Griffin BP, Desai MY. Comparison of severity of aortic regurgitation by cardiovascular magnetic resonance versus transthoracic echocardiography. *Am J Cardiol.* 2011 July 22; [Epub ahead of print].

Garcia J, Kadem L, Larose E, Clavel MA, Pibarot P. Comparison between cardiovascular magnetic resonance and transthoracic doppler echocardiography for the estimation of effective orifice area in aortic stenosis. *J Cardiovasc Magn Reson.* 2011; 13 (1): 25.

Hartung MP, Grist TM, Francois CJ. Magnetic resonance angiography: current status and future directions. *Journal of Cardiovascular Magnetic Resonance.* 2011; 13:19.

Hope MD, Hope TA, Meadows AK, Ordovas KG, Urbania TH, Alley MT, Higgins CB. Bicuspid aortic valve: four-dimensional MR evaluation of ascending aortic systolic flow patterns. *Radiology*. 2010;255(1):53-61.

Keenan, N. G., Mason, J. C., Maceira, A., Assomull, R., O'Hanlon, R., Chan, C., Roughton, M., Andrews, J., Gatehouse, P. D.,

Lara M, Chen CY, Mannor P, Dur O, Menon PG, Yoganathan AP, Pekkan K. Hemodynamics of the hepatic venous three-vessel confluences using particle image velocimetry. *Annals of Biomedical Engineering*. 2011.

Litmanovich D, Bankier A, Cantin L, et al. CT and MRI in diseases of the aorta. *Am J Roentgenology.* 2009;193:928–940.

Liu Q, Lu JP, Wang F, Wang L, Tian JM. Three-dimensional contrast enhanced MR angiography of aortic dissection: a pictorial essay. 2007. *Radiographics*. 27(5): 1311–1321.

Lotz J, Meier C, Leppert A, et al. Cardiovascular flow measurement with phase-contrast MR imaging: basic facts and implementation. *Radiographics.* 2002; 22: 651–71.

M, Hamm B. Noninvasive detection of coronary artery stenoses with multislice computed tomography or magnetic resonance imaging. *Ann Intern Med.* 2006; 145(6): 407-15.

Menke J, Larsen J. Meta-analysis: accuracy of contrast-enhanced magnetic resonance angiography for assessing steno occlusion ins peripheral arterial disease. *Ann Intern Med.* 2010; 153(5): 325-34.

Miller SW, Abbara S, Boxt LM. *Cardiac Imaging: The Requisites, 3rd edition*. Philadelphia: Mosby/Elsevier; 2009: 85-86.

Morita S, Masukawa A, Suzuki K, Hirata M, Kojima S, Ueno E. Unenhanced MR Angiography: Techniques and Clinical Applications in Patients with Chronic Kidney Disease. *Radiographics*. 2011; 31(2):E13–E33.

Muzzarelli S, Meadows AK, Ordovas KG, Hope MD, Higgins CB, Nielsen JC, Geva T, Meadows JJ. Prediction of Hemodynamic Severity of Coarctation by Magnetic Resonance Imaging. *Am J Cardiol.* 2011 Aug 20. [Epub ahead of print].

Nielsen JC, Powell AJ, Gauvreau K, Marcus EN, Prakash A, Geva T. Magnetic resonance imaging predictors of coarctation severity. *Circulation.* 2005; 111(5):622-8.

Nienaber CA, von Kodolitsch Y, Nicolas V, et al. The diagnosis of thoracic aortic dissection by noninvasive imaging procedures. *N Engl J Med* 1993; 328:1 –9.

Pekkan K, Dur O, Sundareswaran K, Kanter K, Fogel M, Yoganatahan A, Undar A. Neonatal aortic arch hemodynamics and perfusion during cardiopulmonary bypass. *J Biomech Eng*. 2008; 130(6):061012.

Perazella MA. Advanced kidney disease, gadolinium and nephrogenic systemic fibrosis: the perfect storm. *Curr Opin Nephrol Hypertens*. 2009; 18: 519-525.

Piccoli G, Slavich G, Gianfagna P, Gasparini D. Cleft bicuspid aortic valve: the Achilles' heel of echocardiography? *Eur Heart Journal.* 2010; 31(17):2140.

Pouleur AC, de Waroux JB, Pasquet A, Watremez C, Vanoverschelde JL, El Khoury G, Gerber BL. Successful repair of quadricuspid aortic valve illustrated by transesophageal echocardiography, 64-slice multidetector computed tomography, and cardiac magnetic resonance. *European Heart Journal*. 2009; 28(22): 2769.

Prakash A, Powell AJ, Krishnamurthy R, Geva T. MRI evaluation of myocardial perfusion and viability in congenital and acquired pediatric heart disease. *Am J Cardiol.* 2004; 93: 657-661.

Sakamoto I, Sueyoshi E, Uetani M. MR imaging of the aorta. *Magn Reson Imaging Clin N Am*. 2010; 18 (1): 43-55.

Scheutz GM, Zacharopoulou NM, Schlattmann P, Dewey M. Meta-analysis: noninvasive coronary angiography using computed tomography versus magnetic resonance imaging. *Ann Intern Med.* 2010; 152(3):167-77.

Schuijf JD, Bax JJ, Shaw LJ, de Roos A, Lamb HJ, van der Wall EE, Wijns W. Meta-analysis of comparative diagnostic performance of magnetic resonance imaging and multislice computed tomography for noninvasive coronary angiography. *Am Heart J.* 2006; 151(2): 404-11.

Secchi F, Iozzelli A, Papini GD, Aliprandi A, Di Leo G, Sardanelli F. MR imaging of aortic coarctation. *Radiol Med.* 2009;114(4):524-37.

Sena L. Cardiac MR imaging: from physics to protocols. *Pediatr Radiol.* 2008; 38(suppl 2): S185-S191.

Shiga T, Wajima Z, Apfel CC, Inoue T, Ohe Y. Diagnostic accuracy of transesophageal echocardiography, helical computed tomography, and magnetic resonance imaging for suspected thoracic aortic dissection: systematic review and meta-analysis. *Arch Intern Med.* 2006;166 :1350 –1356

Taylor AM. Cardiac imaging: MR or CT? Which to use when. *Pediatr Radiol.* 2008; 38 (Suppl 3): S433-S438.

Uretsky S, Supariwala A, Nidadovolu P, Khokar SS, Comeau C, Shubayey O, Campanile F, Wolff SD. Quantification of left ventricular remodeling in response to isolated aortic or mitral regurgitation. *J Cardiovasc Magn Reson.* 2010; 12: 32.

van Dijkman PR, Doornbos J, de Roos A. Improved detection of acute myocardial infarction by magnetic resonance imaging using gadolinium-DTPA. *Int J Card Imaging.* 1989; 5: 1-8.

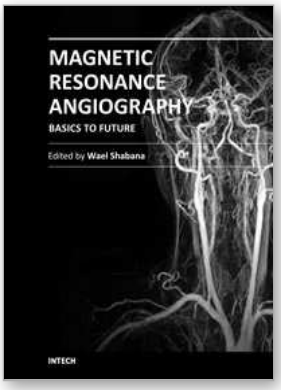


**Magnetic Resonance Angiography Basics to Future**

Edited by Prof. Wael Shabana

ISBN 978-953-51-0401-8
Hard cover, 94 pages
**Publisher** InTech
**Published online** 21, March, 2012
**Published in print edition** March, 2012

As MRI has paved its role in diagnostic angiography. MRA has the potential to provide more physiological and pathophysiological data over the disease in addition to the anatomical information. This book is divided into three sections. The first section discusses the basics of MRI angiography. It starts with focus on the contrast agents that are mainly used in MR angiography with detailed discussion of advantage and limitations of different types of contrast. The second chapter is oriented more towards the technical consideration that contribute to good quality examination, both the non contrast and contrast based sequences from black to bright blood imaging , contrast enhanced MRA, review of clinical application of MRA in different body systems and MR venography. The second section reviews the clinical application of MRI mainly in the head and neck and brain ischemia imaging. The new high resolution intracranial plaque imaging of the branch athermanous disease, to the hemodynamic of intracranial atherosclerotic stroke and quantitative MRA imaging in neurovascular imaging, are the topics in this section. Also this section covers the future prospective and the new frontiers MRI angiography is exploring. In the third section, MRA of aortic disease in children with emphasis on cardiac MRA.

**How to reference**

In order to correctly reference this scholarly work, feel free to copy and paste the following:

Shobhit Madan, Soma Mandal and Sameh S. Tadros (2012). Magnetic Resonance Angiography of Aortic Diseases in Children, Magnetic Resonance Angiography Basics to Future, Prof. Wael Shabana (Ed.), ISBN: 978-953-51-0401-8, InTech, Available from: http://www.intechopen.com/books/magnetic-resonance-angiography-basics-to-future/magnetic-resonance-angiography-of-aortic-diseases-in-children

INTECH
open science | open minds

**InTech Europe**
University Campus STeP Ri
Slavka Krautzeka 83/A
51000 Rijeka, Croatia
Phone: +385 (51) 770 447
Fax: +385 (51) 686 166
www.intechopen.com

**InTech China**
Unit 405, Office Block, Hotel Equatorial Shanghai
No.65, Yan An Road (West), Shanghai, 200040, China
中国上海市延安西路65号上海国际贵都大饭店办公楼405单元
Phone: +86-21-62489820
Fax: +86-21-62489821